Supporting Information

Dual-Functional Cr^{3+}-doped Far-Red to NIR Broadband Phosphors Enabling High-Fidelity White Lighting and Non-Destructive Detection

Zhenwei Jia,[a] Jingyi Gao,[a] Xiaohui Zhao,[a] Mengdi Yue,[a] Li Wu,[a*] Yongfa Kong[a] and Jingjun Xu[a]

[a] Key Laboratory of Weak-Light Nonlinear Photonics, Ministry of Education, School of Physics, Nankai University, Tianjin 300071, China.

[*] E-mail: lwu@nankai.edu.cn

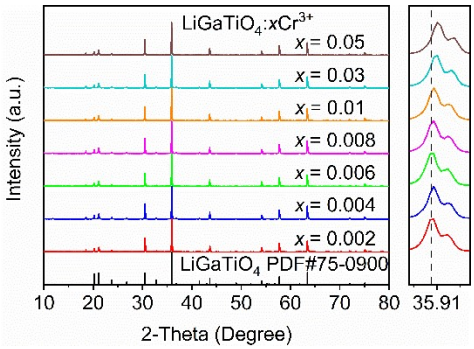

Fig. S1. XRD patterns of LGT:xCr^{3+} (x = 0.002, 0.004, 0.006, 0.008, 0.01, 0.03, 0.05).

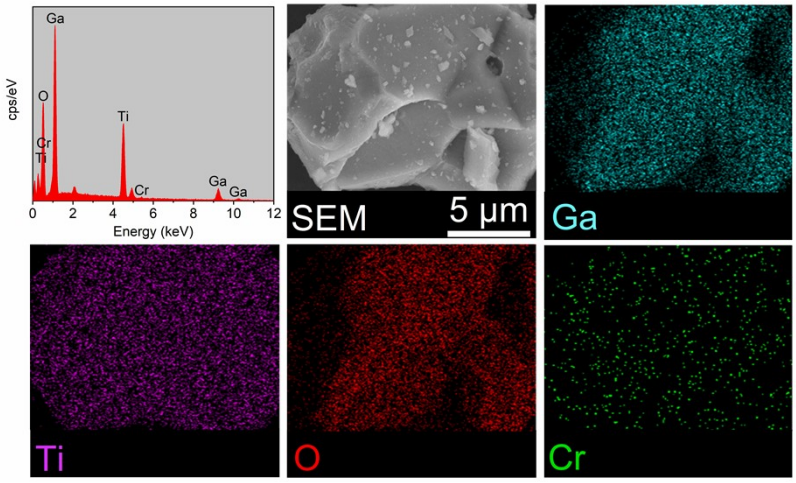

Fig. S2. SEM, EDS and elemental mapping of LGT:0.008Cr^{3+}.

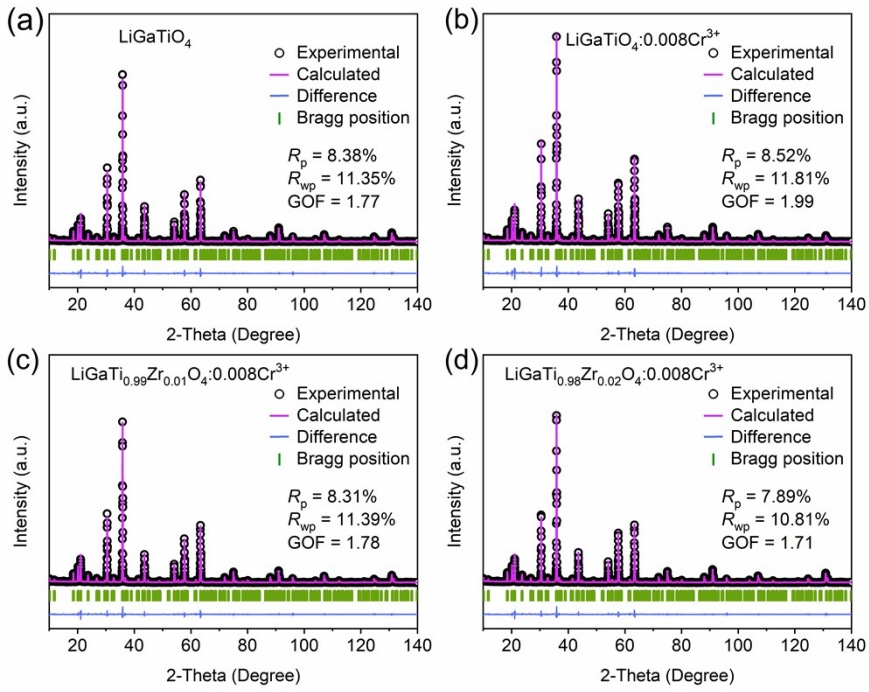

Fig. S3. Rietveld refinement results of (a) LGT, (b) LGT:0.008Cr^{3+}, (c) $LiGaTi_{0.99}Zr_{0.01}O_4$:0.008$Cr^{3+}$ and (d) $LiGaTi_{0.98}Zr_{0.02}O_4$:0.008$Cr^{3+}$.

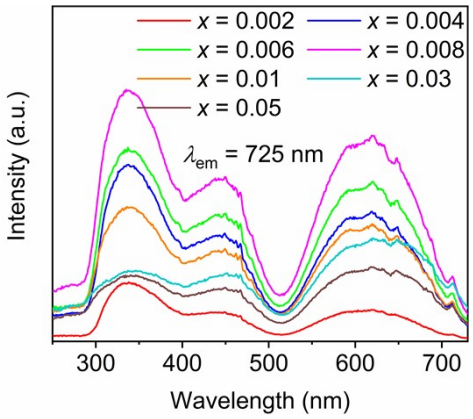

Fig. S4. PLE spectra of LGT:xCr^{3+}(x = 0.002, 0.004, 0.006, 0.008, 0.01, 0.03, 0.05).

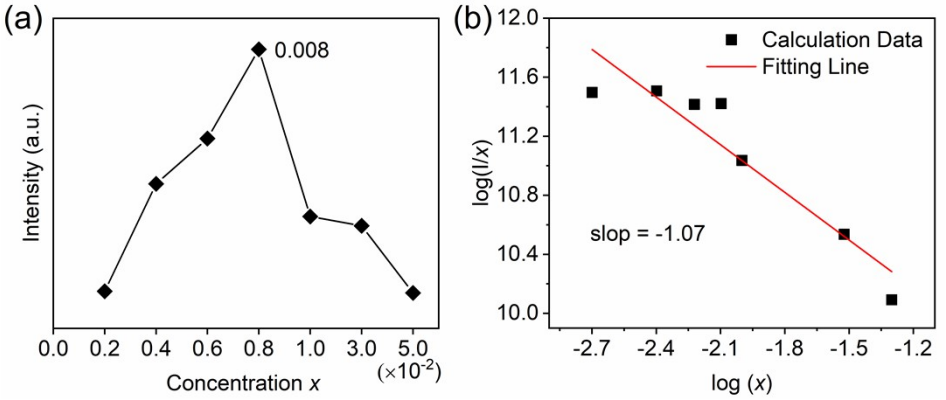

Fig. S5. (a) The relative intensity of LGT:xCr^{3+}(x = 0.002, 0.004, 0.006, 0.008, 0.01, 0.03, 0.05). (b) The fitting results between log(I/x) and log(x).

The critical energy transfer distance R_c was calculated from the equation $R_c = 2(\frac{3V}{4\pi X_c N})^{\frac{1}{3}}$, where V is the cell volume, X_c is the critical concentration of Cr^{3+}, and N is the cation number that Cr^{3+} could occupy in per unit cell. For LGT:xCr^{3+}, V = 856.74 Å^3, N = 16, X_c = 0.008, and the R_c value is determined to be 23.4 Å. The calculation result is greater than 5 Å, which means that the multipolar interactions lead to concentration quenching in LGT:xCr^{3+}. The mechanism of multipolar interactions between Cr^{3+} ions can be further explained using the formula $\frac{I}{x} = k\left[1 + \beta(x)^{\frac{\theta}{3}}\right]^{-1}$, where I is the emission intensity of the sample, x is the concentration of Cr^{3+} ion, k and β are constants. The value of θ is 3 corresponds to the energy transfer among the nearest-neighbor ions, while 6, 8 and 10 corresponds to dipole–dipole, dipole–quadrupole and quadrupole–quadrupole interactions, respectively. Fig S4 shows the relation between log(I/x) and log(x), and the value is equals to 3.21, which is close to 3. Therefore, the main concentration quenching mechanism for LGT:xCr^{3+} is the energy transfer among the nearest-neighbor ions.

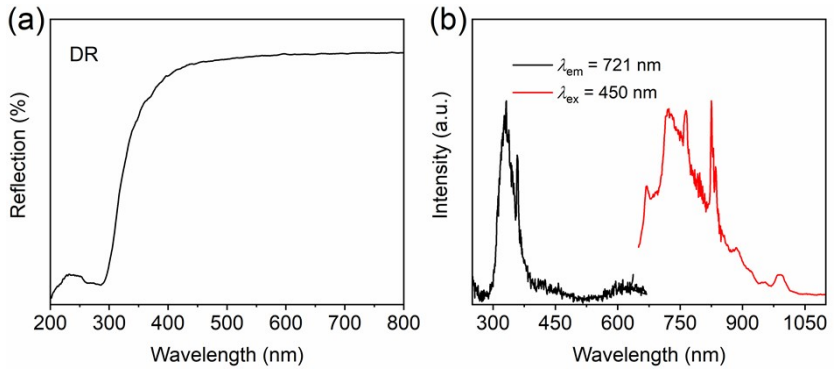

Fig. S6. Fitting results of the fluorescence decay curve for LGT:0.008Cr^{3+} phosphors, monitoring 725 nm at room temperature.

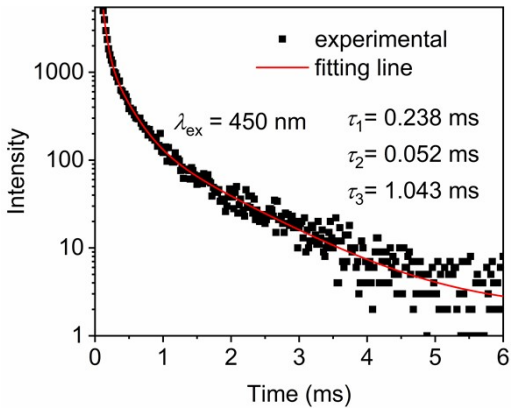

Fig. S7. Fitting results of the fluorescence decay curve for LGT:0.008Cr^{3+} phosphors, monitoring 725 nm at room temperature.

The decay time is fitted well with the triple-exponential function $I_t = I_0 + \sum_{i=1}^{3} A_i \exp(-\frac{t}{\tau_i})$, where I_t relates to the luminescent intensity at time t, I_0 and A_i are constants, τ_i is the lifetime of different emission centers.

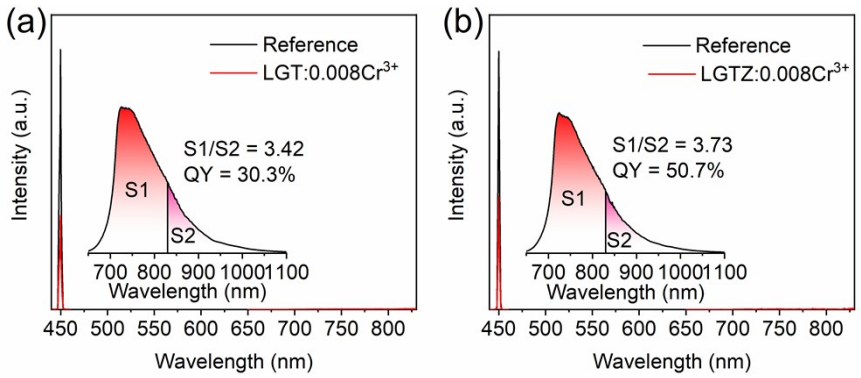

Fig. S8. QY of LGT:0.008Cr^{3+} phosphors and LGTZ:0.008Cr^{3+}.

The AE (absorption efficiency), IQE (internal quantum efficiency), and EQE (external quantum efficiency) can be obtained by the following equations:

$$IQE = \frac{\int L_s}{\int E_r - \int E_s} \#(S1)$$

$$AE = \frac{E_r - E_s}{E_r} \#(S2)$$

$$EQE = AE * IQE \#(S3)$$

Where L_s is the luminescence spectrum of the sample, and E_s and E_r are the excitation spectra with and without the sample in the integrating sphere, respectively. The QY here refers to the IQE defined in Eq. (S1).

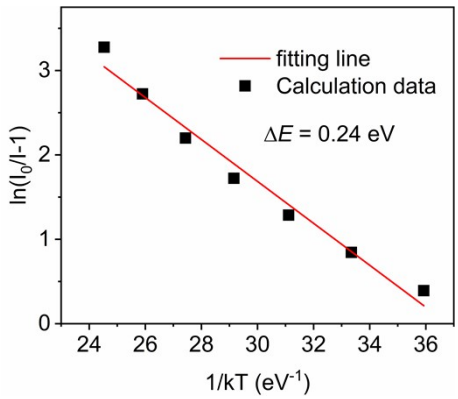

Fig. S9. The relationship between ln(I_0/I-1) and 1/kT of LGT:0.008Cr^{3+}.

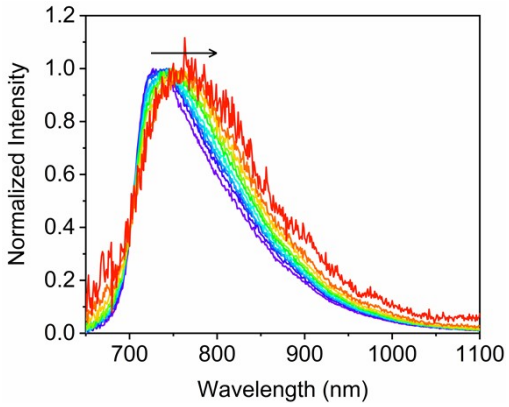

Fig. S10. Normalized temperature dependent PL spectra properties of LGTZ:0.008Cr^{3+}.

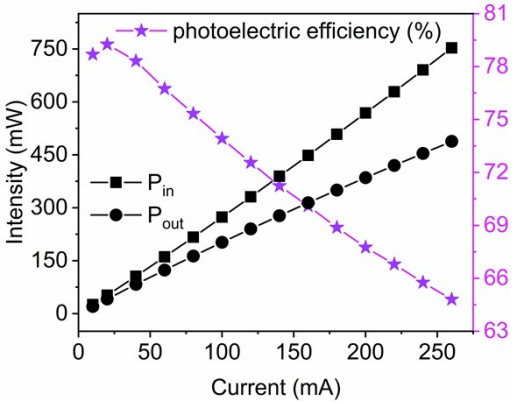

Fig. S11. The output power and photoelectric efficiency of 450 nm LED chip with input current.

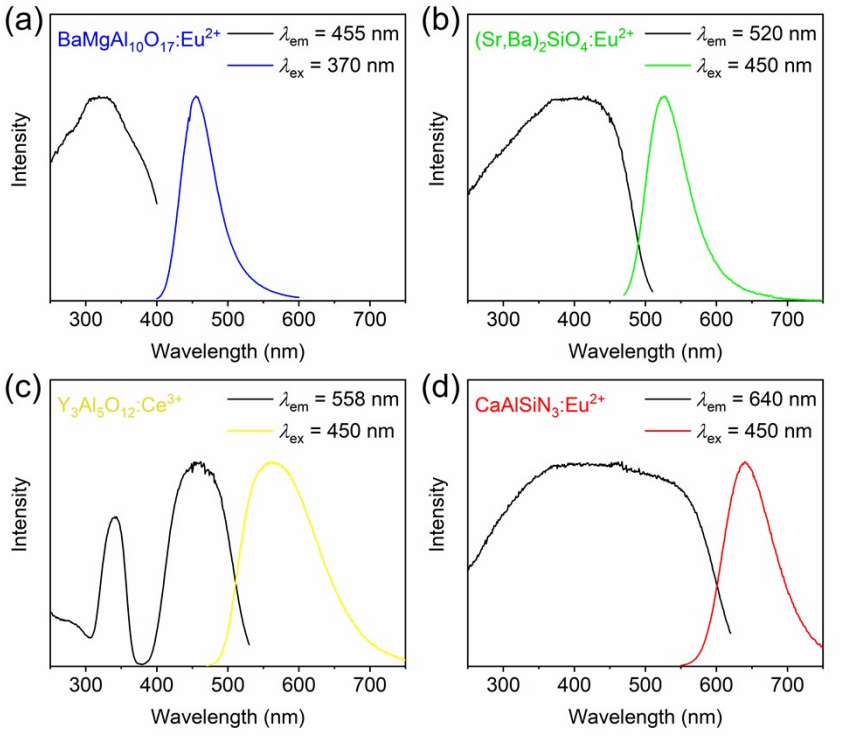

Fig. S12. PLE and PL spectra of commercial phosphors: (a) $BaMgAl_{10}O_{17}:Eu^{2+}$, (b) $(Sr,Ba)_2SiO_4:Eu^{2+}$, (c) $Y_3Al_5O_{12}:Ce^{3+}$, and (d) $CaAlSiN_3:Eu^{2+}$.

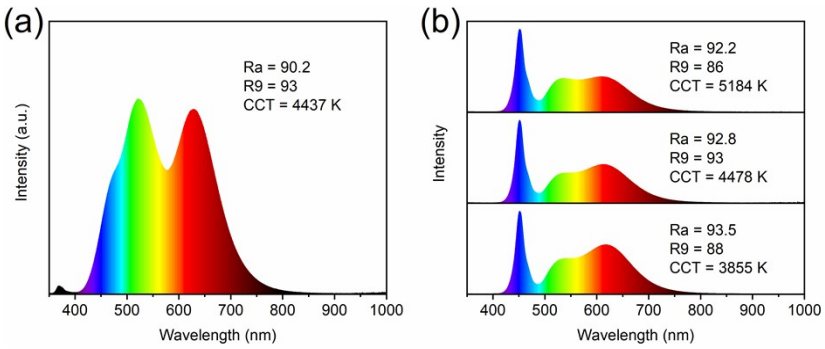

Fig. S13. (a) EL spectra of fabricated UV-pumped white pc-LED device utilizing blended RGB commercial phosphors. (b) EL spectra of fabricated blue-pumped white pc-LED device utilizing blended GYR commercial phosphors.

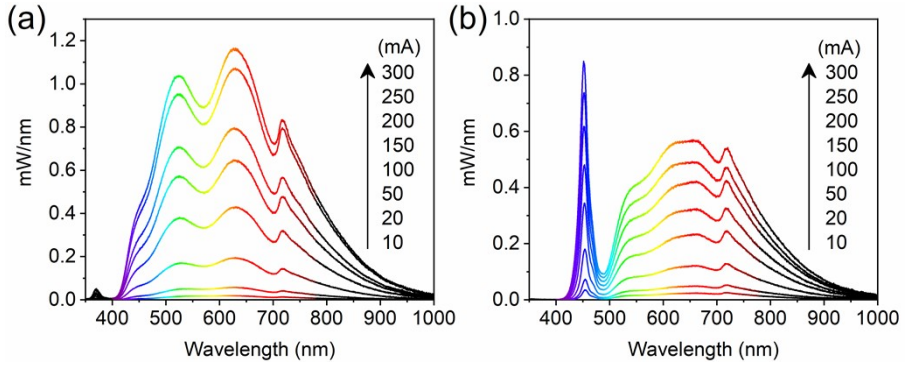

Fig. S14. (a) EL spectra of fabricated UV-based white pc-LED device at varied current over 10-300 mA. (b) EL spectra of fabricated blue-based white pc-LED device at varied current over 10-300 mA.

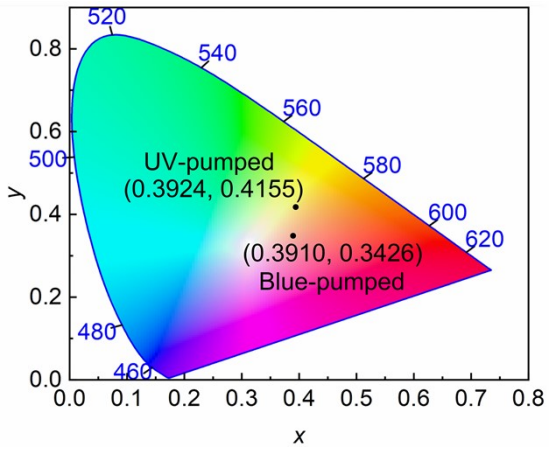

Fig. S15. CIE chromaticity coordinates of UV-pumped and blue-pumped white pc-LEDs.

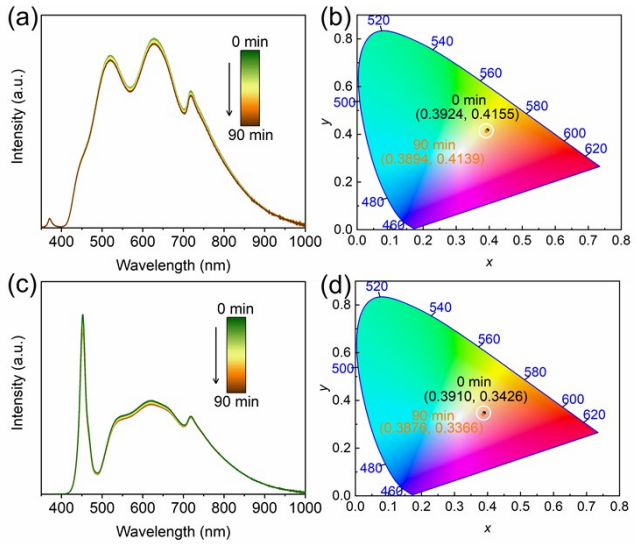

Fig. S16. (a) Photobleaching spectra and (b) CIE diagram of the UV-pumped white pc-LED recorded within 90 min of operation; (c) photobleaching spectra and (d) CIE diagram of the blue-pumped white pc-LED recorded within 90 min of operation.

Table S1. Lattice parameters and agreement factors for $LiGaTiO_4$, $LiGaTiO_4$:0.008Cr^{3+}, $LiGaTi_{0.99}Zr_{0.01}O_4$:0.008$Cr^{3+}$, $LiGaTi_{0.98}Zr_{0.02}O_4$:0.008$Cr^{3+}$ and $LiGaTi_{0.97}Zr_{0.03}O_4$:0.008$Cr^{3+}$ refined by Rietveld method.

Formula	$LiGaTiO_4$	$LiGaTiO_4$:0.008 Cr^{3+}	$LiGaTi_{0.99}Zr_{0.01}$ O_4:0.008Cr^{3+}	$LiGaTi_{0.98}Zr_{0.02}$ O_4:0.008Cr^{3+}	$LiGaTi_{0.97}Zr_{0.03}$ O_4:0.008Cr^{3+}
Crystal system	Orthorhombic	Orthorhombic	Orthorhombic	Orthorhombic	Orthorhombic
Space group	Imma	Imma	Imma	Imma	Imma
a (Å)	5.8736(4)	5.8702(4)	5.8732(5)	5.8743(4)	5.8734(5)
b (Å)	17.6020(12)	17.6024(12)	17.5986(14)	17.6030(12)	17.6051(14)
c (Å)	8.2917(6)	8.2913(6)	8.2935(7)	8.2938(6)	8.2979(7)
α=β=γ (°)	90	90	90	90	90
Z	12	12	12	12	12
Volume ($Å^3$)	857.25(11)	856.74(10)	857.23(12)	857.62(10)	858.02(12)
R_p	8.38	8.76	8.31	7.89	7.98
R_{wp}	11.35	12.22	11.39	10.81	10.87
R_{exp}	6.4	5.92	6.38	6.32	6.50
GOF	1.77	2.06	1.78	1.71	1.67

Table S2. Atomic positions and occupancies for $LiGaTiO_4$ refined by Rietveld method.

	Np	*x*	*y*	*z*	Occupancy
Ga1	8	0.00000	0.171(17)	0.50000	0.25
Ga2	8	0.25000	0.085(10)	0.25000	0.25
Ga3	8	0.00000	0.0834(7)	0.87500	1.0
Ti1	8	0.00000	0.173(9)	0.50000	0.75
Ti2	8	0.25000	0.079(5)	0.25000	0.75
Li1	4	0.00000	0.00000	0.50000	1.0
Li2	4	0.25000	0.25000	0.75000	1.0
Li3	4	0.75000	0.25000	0.75000	1.0
O1	16	0.24000	0.40000	0.00000	1.0
O2	8	0.00000	0.00000	0.25000	1.0

O3	8	0.00000	0.150(2)	0.25000	1.0
O4	8	0.00000	0.167(2)	0.75000	1.0
O5	8	0.25000	0.25000	0.00000	1.0

Table S3. Atomic positions and occupancies for $LiGaTiO_4$:0.008Cr^{3+} refined by Rietveld method.

	Np	*x*	*y*	*z*	Occupancy
Ga1	8	0.00000	0.17(2)	0.50000	0.249(8)
Cr1		0.00000	0.17(2)	0.50000	0.001(8)
Ga2	8	0.25000	0.062(2)	0.25000	0.243(8)
Cr2		0.25000	0.062(2)	0.25000	0.007(8)
Ga3	8	0.00000	0.0860(6)	0.87500	1.0
Ti1	8	0.00000	0.171(11)	0.50000	0.75
Ti2	8	0.25000	0.0870(12)	0.25000	0.75
Li1	4	0.00000	0.00000	0.50000	1.0
Li2	4	0.25000	0.25000	0.75000	1.0
Li3	4	0.75000	0.25000	0.75000	1.0
O1	16	0.24000	0.40000	0.00000	1.0
O2	8	0.00000	0.00000	0.25000	1.0
O3	8	0.00000	0.147(3)	0.25000	1.0
O4	8	0.00000	0.168(2)	0.75000	1.0
O5	8	0.25000	0.25000	0.00000	1.0

Table S4. Atomic positions and occupancies for $LiGaTi_{0.99}Zr_{0.01}O_4$:0.008$Cr^{3+}$ refined by Rietveld method.

	Np	*x*	*y*	*z*	Occupancy

Ga1	8	0.00000	0.170(2)	0.50000	0.25
Ga2	8	0.25000	0.084(12)	0.25000	0.25
Ga3	8	0.00000	0.0824(8)	0.87500	1.0
Ti1	8	0.00000	0.173(12)	0.50000	0.74(2)
Zr1		0.00000	0.173(12)	0.50000	0.01(2)
Ti2	8	0.25000	0.079(7)	0.25000	0.74(2)
Zr2		0.25000	0.079(7)	0.25000	0.00(2)
Li1	4	0.00000	0.00000	0.50000	1.0
Li2	4	0.25000	0.25000	0.75000	1.0
Li3	4	0.75000	0.25000	0.75000	1.0
O1	16	0.24000	0.40000	0.00000	1.0
O2	8	0.00000	0.00000	0.25000	1.0
O3	8	0.00000	0.151(3)	0.25000	1.0
O4	8	0.00000	0.165(3)	0.75000	1.0
O5	8	0.25000	0.25000	0.00000	1.0

Table S5. Atomic positions and occupancies for $LiGaTi_{0.98}Zr_{0.02}O_4$:$0.008Cr^{3+}$ refined by Rietveld method.

	Np	*x*	*y*	*z*	Occupancy
Ga1	8	0.00000	0.169(12)	0.50000	0.25
Ga2	8	0.25000	0.088(5)	0.25000	0.25
Ga3	8	0.00000	0.0822(7)	0.87500	1.0
Ti1	8	0.00000	0.173(6)	0.50000	0.73(19)
Zr1		0.00000	0.173(6)	0.50000	0.02(19)
Ti2	8	0.25000	0.079(7)	0.25000	0.75(19)
Zr2		0.25000	0.079(7)	0.25000	0.00(19)

Li1	4	0.00000	0.00000	0.50000	1.0
Li2	4	0.25000	0.25000	0.75000	1.0
Li3	4	0.75000	0.25000	0.75000	1.0
O1	16	0.24000	0.40000	0.00000	1.0
O2	8	0.00000	0.00000	0.25000	1.0
O3	8	0.00000	0.151(3)	0.25000	1.0
O4	8	0.00000	0.164(3)	0.75000	1.0
O5	8	0.25000	0.25000	0.00000	1.0

Table S6. Atomic positions and occupancies for $LiGaTi_{0.97}Zr_{0.03}O_4$:0.008$Cr^{3+}$ refined by Rietveld method.

	Np	*x*	*y*	*z*	Occupancy
Ga1	8	0.00000	0.165(3)	0.50000	0.25
Ga2	8	0.25000	0.08(4)	0.25000	0.25
Ga3	8	0.00000	0.0805(6)	0.87500	1.0
Ti1	8	0.00000	0.1801(16)	0.50000	0.725(2)
Zr1		0.00000	0.1801(16)	0.50000	0.025(2)
Ti2	8	0.25000	0.08(2)	0.25000	0.745(2)
Zr2		0.25000	0.08(2)	0.25000	0.005(2)
Li1	4	0.00000	0.00000	0.50000	1.0
Li2	4	0.25000	0.25000	0.75000	1.0
Li3	4	0.75000	0.25000	0.75000	1.0
O1	16	0.24000	0.40000	0.00000	1.0
O2	8	0.00000	0.00000	0.25000	1.0
O3	8	0.00000	0.147(3)	0.25000	1.0
O4	8	0.00000	0.162(3)	0.75000	1.0

O5	8	0.25000	0.25000	0.00000	1.0

Table S7. The calculated distortion index D and the variance σ^2.

		0	0.03
Ga1-O	d_{av}	2.02855	2.03034
	D_1	0.02005	0.03913
	σ^2_1	39.40317	46.16915
Ga2-O	d_{av}	2.01518	2.00799
	D_2	0.04637	0.05069
	σ^2_2	44.85236	52.56347

Table S8. The CIE chromaticity coordinates and color purity of the NIR pc-LED under different driving currents.

Current (mA)	Voltage (V)	Power (mW)	T (℃)	CIE (x, y)	Color purity (%)
10	2.556	25.56	24.6	(0.7331, 0.2669)	89.5
20	2.587	51.74	25.1	(0.7329, 0.2671)	94.2
50	2.644	132.2	26.6	(0.7328, 0.2672)	94.3
100	2.712	271.2	28.2	(0.7328, 0.2672)	94.6
150	2.77	415.5	31.3	(0.7328, 0.2672)	94.6
200	2.825	565	35.4	(0.7328, 0.2672)	94.6
250	2.875	718.75	37.9	(0.7328, 0.2672)	94.3
300	2.923	876.9	41.7	(0.7328, 0.2672)	94.5